ECS Journal of Solid State Science and Technology, **3** (2) N1-N6 (2014)
2162-8769/2014/3(2)/N1/6/$31.00 © The Electrochemical Society

Characterization of Lanthanum-Aluminum Oxide Thin Films Deposited by Spray Pyrolysis

A. N. Meza-Rocha,[a,z] E. Zaleta-Alejandre,[a] J. G. Cabañas-Moreno,[b] S. Gallardo-Hernández,[a] Z. Rivera-Álvarez,[a] M. Aguilar-Frutis,[c] and C. Falcony[a]

[a]*Departamento de Física, CINVESTAV IPN. Apdo. 7000 México DF, México*
[b]*Programa de Doctorado en Nanociencias y Nanotecnología, CINVESTAV IPN, A., México DF 07360, México*
[c]*CICATA-IPN, Legaria 694 Colonia Irrigación, C.P. 11500, México, Distrito Federal, México*

The optical, electrical, and structural characteristics of lanthanum-aluminum oxide thin films deposited by ultrasonic spray pyrolysis are presented. The films were deposited using a lanthanum nitrate and aluminum acetylacetonate solution in N, N-dimethylformamide on (100) Si substrates. The substrate temperature during deposition was in the 500–650°C range. The deposition activation energy was in the range of 17.4–20 kJ mol^{-1}, depending on the relative concentration of lanthanum to aluminum in the precursor solution. The films were amorphous even at 650°C and they were given no further temperature annealing. The refractive index at 630 nm was in the range of 1.70–1.755 depending on the amount of lanthanum in the films. The electrical characteristics of the films were determined from capacitance and current versus voltage measurements of metal-oxide-semiconductor (MOS) structures incorporating them. A dielectric constant in the range of 5.2–10, and interface states density of the order of 10^{11}-10^{12} eV^{-1} cm^{-2} were measured. Their electrical breakdown field was in the range of 4.5–7.6 $MVcm^{-1}$ for films deposited at 500 and 550°C and a thickness under 43 nm.
© 2013 The Electrochemical Society. [DOI: 10.1149/2.013402jss] All rights reserved.

Manuscript submitted September 9, 2013; revised manuscript received October 29, 2013. Published December 5, 2013. This was Paper 1906 presented at the Boston, Massachusetts, Meeting of the Society, October 9–14, 2011.

Dielectric oxides such as Al_2O_3, HfO_2, ZrO_2, La_2O_3 among others, have received considerable attention over the years for metal oxide semiconductor field effect transistors (MOSFET) and metal insulator metal capacitors (MIM) applications due to their high band gaps and high dielectric constants (k).[1] Lanthanum oxide (La_2O_3) has been considered as candidate for gate dielectrics applications because its high dielectric constant (k ≈ 27), low leakage current, relative large bandgap (E_g = 5.8 eV), and high band offset with respect to silicon.[2] However, it is well known that La_2O_3 is hygroscopic, and has poor thermal stability and poor interface properties which deteriorates its dielectric properties reducing the k value, generating positive fixed charges, increasing the leakage current density and the flatband voltage shift,[3,4] leading to undesirable electrical characteristic. A solution for this problem is modifying the material properties of La_2O_3 by introducing foreign atoms such as silicon, aluminum and nitrogen into the bonding networks.[3] Aluminum oxide (Al_2O_3) has also been considered for gate dielectric applications because it has a large E_g = 5.6 eV, a k value of 9 to 10, and good thermal stability.[5,6] Another important characteristic of aluminum oxide films is that they remain amorphous even at high deposition temperatures with excellent electrical characteristics.[6] A possible solution would be to combine it with La_2O_3 to improve the chemical and electrical characteristics of both oxides.[3] Lanthanum aluminum oxide (hereafter referred as LA) films have been deposited previously by atomic layer deposition (ALD), pulsed laser deposition (PLD), and molecular beam epitaxy (MBE), among other techniques.[2,5,7] In this work, LA films have been synthesized by the ultrasonic spray pyrolysis technique, a very simple and relatively cost-effective processing method because it does not require expensive vacuum techniques and still yields excellent electronic quality films, as in the case of aluminum and yttrium oxide thin films.[6,8,9] The spray pyrolysis technique has several on site reaction regimes, depending on the type of precursors, the speed at which they arrive to hot substrate and the temperature of substrate.[10,11] One of these regimes mimics CVD process in which the radiation heat from the substrate evaporate the solvent in the droplet and also evaporates the precursor, in such way that vapors of the precursor arrive to the substrate surface and react pretty much as in the case of CVD process. Under this condition, the advantages of CVD technique are extrapolated to the spray pyrolysis technique. This is case for the precursors using in this work in which under the condition chosen for deposition of the films we fall within this deposition regime.[6,8] There are possibilities to be explored, for reducing the final thickness of the deposited films as well to have a better control of the interface with the substrate that will open the applicability of this technique on device manufacturing. It should be pointed out that to the best authors knowledge there are scarce reports on LA films deposited by ultrasonic spray pyrolysis in the literature.[12]

Experimental

The LA thin films were deposited by the ultrasonic spray pyrolysis technique using a spraying solution made with aluminum acetylacetonate ($Al(acac)_3$) and lanthanum(III) nitrate hydrate $La(NO_3)_3xH_2O$ dissolved in N,N-Dimethylformamide. The experimental arrangement includes two ultrasonic generators operated at 1.2 MHz for the formation of an aerosol from the spraying solution; compressed air was used as carrier gas with a flow rate of 10 l min^{-1} for each ultrasonic generator. In order to investigate the effect of the precursors on the deposition process, two different solutions with lanthanum nitrate/aluminum acetylacetonate molarity ratios of 0.025/0.0025 and 0.02625/0.00125 (hereafter referred as LA1 and LA2, respectively) were used. The incorporation of aluminum and lanthanum into the film depends on the precursor concentration rate and on the deposition temperature as well, the concentration ratios used in this work were chosen to obtain an incorporation of La higher than 10 at% by EDS (line M) which were also the ones to obtain the best results in terms of the electrical characterization. The films were deposited on n-type (100) silicon substrates with a resistivity of 0.1Ω-cm and 1000 Ω-cm for electrical and structural characterization, respectively. The silicon substrates were given the standard RCA cleaning procedure before the deposition process. Substrate temperatures during deposition were in the range of 500–650°C. The thickness and refractive index of the films were measured with a single wavelength ellipsometer (Gaertner, L117, λ = 632.8 nm). The X-ray diffraction (XRD) patterns were recorded using Cu Kα (α = 1.541 Å) radiation with 2θ values ranging from 20° to 90° in a SIEMENS D-500 X-ray diffractometer. Cross section samples were prepared by the Focused Ion Beam technique (FIB). The cross section structures were analyzed by Scanning Electron Microscope operated in STEM mode. The chemical composition analysis was performed by energy dispersion spectroscopy (EDS) with a scanning electron microscope (JEOL, JMS-7800F). The surface roughness was measured with a Park Scientific Instruments atomic force microscope. Elemental depth profiles studies were carried out by secondary ion mass spectroscopy (SIMS) employing a CAMECA 6F using cesium for primary beam. The capacitance vs. voltage (C-V) and current vs. voltage (I-V) measurements were

[z]E-mail: ameza@fis.cinvestav.mx

Downloaded on 2016-09-12 to IP 130.203.136.75 address. Redistribution subject to ECS terms of use (see ecsdl.org/site/terms_use) unless CC License in place (see abstract).
IPR2025-00845
Apple-Sony EX1080 Page 1

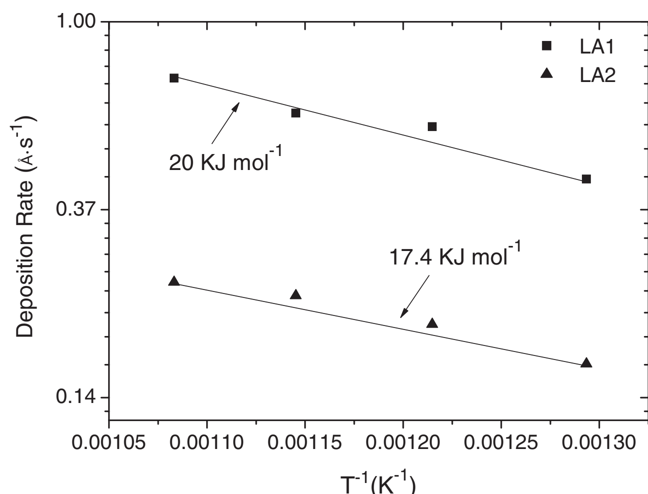

Figure 1. Arrhenius plot of deposition rate vs. T^{-1} for the two types of samples deposited.

performed in an automated equipment by Keithley instruments. For this purpose the films were integrated into MOS structures. Aluminum metal contacts were thermally evaporated on top of the films with an area of 1.5 and 2.2 × 10^{-2} cm^{-2} for this purpose.

Results and Discussion

The activation energy of the deposition process for the LA films was obtained plotting the deposition rate (D) as function of the reciprocal substrate temperature (T^{-1}) in a semilogarithmic scale and fitting a line to the data. Figure 1 shows this type of plot for films LA1 and LA2, it is observed in both cases that the deposition rate follows an exponential relation D ∼ exp(-E_a/RT). The dependence of the thickness on deposition temperature indicates that the process of deposition of the films on Si is surface reaction controlled.[13] From the slope of the line fitted activation energies of 20 and 17.4 kJ mol^{-1} for LA1 and LA2, respectively, were determined. The activation energies calculated for both solutions are similar which indicate that the type of deposition process is limited by the reaction at the substrate surface of the arriving precursors. These values are in the range of activation energies reported for aluminum and lanthanum oxide films deposited by spray pyrolysis and liquid injection MOCVD, respectively.[6,14]

Figure 2 shows a typical view of the surface topography for LA1 (a) and LA2 (b) films deposited at 550°C. The average roughness, calculated on a 1 μm^2 area, was in all cases less than 8 Å without any dependence on deposition temperature. The low roughness suggests that the deposited films follow the topography of silicon which has a low roughness (∼8 Å) to start with. It should be pointed out that smooth films are desirable for dielectric applications because its low roughness leads to an excellent interface with the metallic contact when they are incorporated into an MOS structure, due to the fact that thermal evaporation is capable to planarizing by filling the gaps on the film surface roughness. However, if these gaps are filled, once an electric field is applied they will appear as spikes which will produce a non-uniform electric field across the films which could result on a low electrical field breakdown.

Figure 3 shows the SIMS elemental profiles for LA1 and LA2 deposited at 500 and 650°C. In all cases, it is observed the presence of Si atoms on the surface which are likely diffused out of the silicon substrate to the surface during the deposition process. The increment of the relative counts of Si atoms on the film surface with temperature suggests that the diffusion of Si atoms could be related, at least in part, with a temperature related process. The actual mechanism that gives rise to this diffusion is not clear, however, we suppose that during the first stage of the deposition process the silicon atoms start

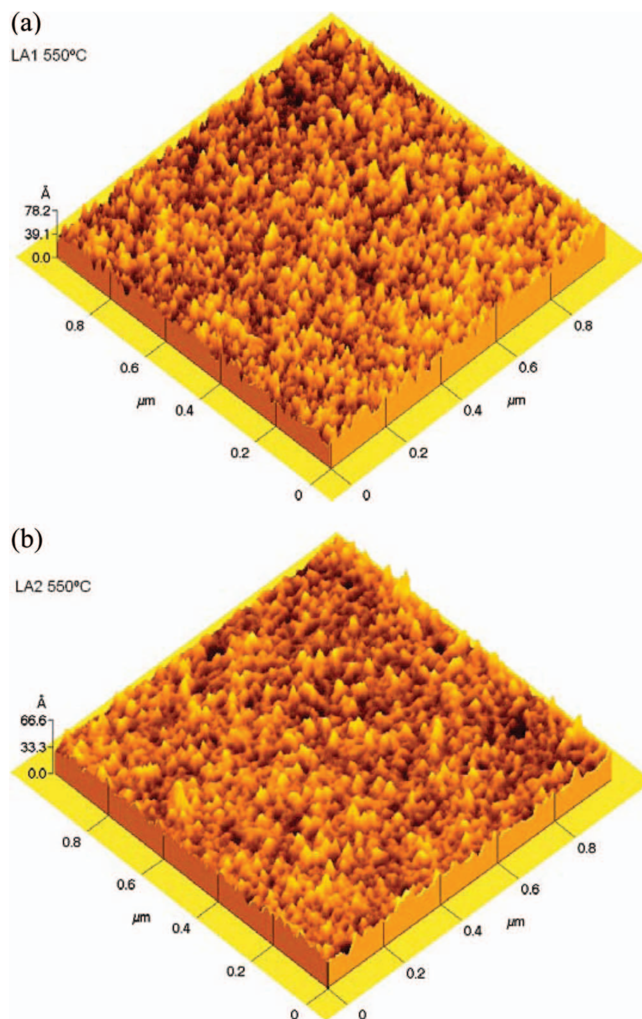

Figure 2. Typical AFM image for films deposited at 550°C.

to move gradually as the films is growing without binding with La and/or Al to accommodate finally on the films surface. This type of behavior has been observed previously in Al_2O_3 and La_2O_3 thin films deposited by pulsed spray pyrolysis and cyclic chemical vapor deposition, respectively.[15,16] The possibility that silicon detected on the film surface could be related to pinholes or porosity reaching down to the substrate has been ruled out since in this case a constant distribution of silicon across the film thickness would be expected. It is also observed that the content of lanthanum through the films is not uniform, after a spike at the film surface, the lanthanum content goes to a low value and recovers to a slightly higher value. The explanation for such spike on the surface films could be associated to an instrumental transient due to preferential sputtering, where heavier elements (La) stay on the surface by a longer time than lighter ones (Al, O). The oxygen has a fairly constant presence throughout the film thickness for films deposited at 650°C, but films deposited at 500°C show a higher concentration near the film surface and a gradual decrease toward the interface with the substrate. Also, higher deposition temperature increases the signal associated with lanthanum content indicating a more efficient incorporation of lanthanum in the film; this could be due to a better decomposition of the lanthanum precursor ($La(NO_3)_3XH_2O$) which is completely decomposed into La_2O_3 at temperatures higher than 650°C.[17] The content of carbon was not quantified in this work but its presence has been documented in previous work related with the use of acetylacetonate precursors for metal oxides deposition.[18] It has been determined that the amount of carbon remaining in the films is less than 5 at% including that carbon that could be related to

Downloaded on 2016-09-12 to IP 130.203.136.75 address. Redistribution subject to ECS terms of use (see ecsdl.org/site/terms_use) unless CC License in place (see abstract).
IPR2025-00845
Apple-Sony EX1080 Page 2

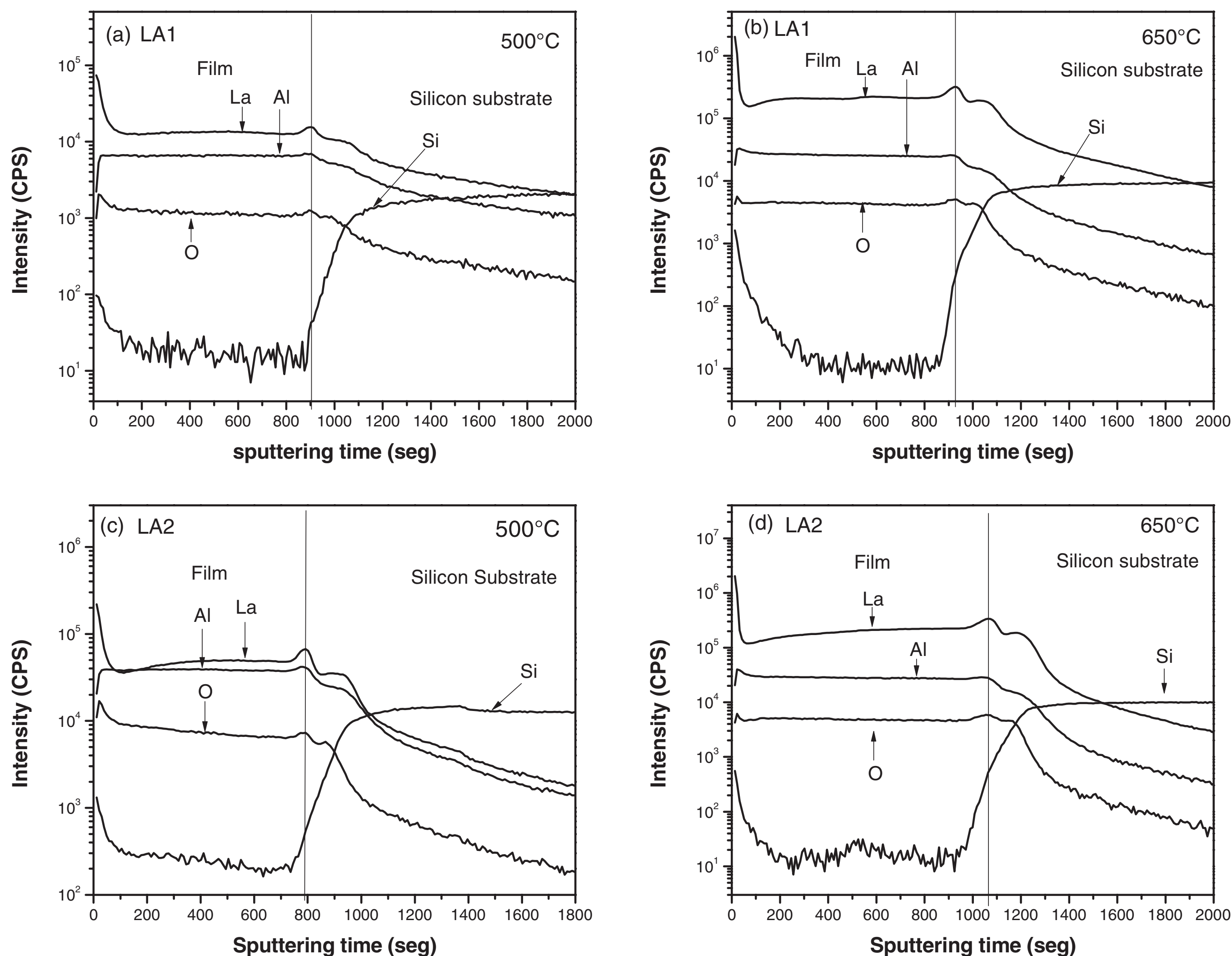

Figure 3. Elemental depth profile for films deposited at 500 and 650°C.

post-deposition contamination. Regarding, the presence of nitrogen, it was not detected by either EDS or SIMS. Therefore, it is likely that the lanthanum nitrate that was not decomposed during the deposition do not remain into the films. At the interface with the Si substrate, there is a transitional interface layer in which an inter-diffusion of La and Al into the Si substrate as well as an out-diffusion of Si are observed. This interfacial layer might be composed by SiO_x and (Al, La)-Silicates species. The formation of (Al, La)-Silicate species could originate during the deposition process by oxidation of the silicon surface and/or a reaction between silicon and the LA film.[19] In the presence it was not possible to determine the bound state of the elements detected but in previous work using XPS on similar type of structures, it has been observed the formation of (Al, La)-Silicates. Therefore, it is assumed that in the present case is similar situation occurs; the formation of the (Al, La)-Silicate layer has been observed in $LaAlO_3$, Al_2O_3 and La_2O_3 films deposited by laser molecular beam epitaxy, atomic layer deposition, metal organic vapor deposition and pyrolysis method.[19–23] SIMS measurement can be used to determine the interface thickness in term of sputter time. The sputter time in the interface layer for LA1 films deposited at 500 and 650°C was 61 and 89 seconds, respectively, while for LA2 films deposited at 500 and 650°C was 61 and 91 seconds, respectively. If we assume that the deposition rate changes at 500 and 650°C are negligible, the films deposited at 650°C have an interfacial layer thicker than those deposited at 500°C regardless of the solution composition. The presence of an interfacial layer is not desirable for MOS applications due to reduction of the dielectric constant effective value; however, in some cases this layer reduces the interfacial density states leading to better interface characteristics.[9] The films were amorphous at temperatures up to 650°C, within the resolution of the X-ray diffractometer (data not shown), this behavior is similar to that previously observed for Al_2O_3, La_xAl_yO and La_2O_3.[6,24,25] This structural characteristic is desirable for CMOS applications because the leakage current tends to increase along the grain boundaries of crystallized films. Besides, it is easier to deposit amorphous films by low cost methods like spray pyrolysis than more expensive ones like atomic layer deposition (ALD) and molecular beam epitaxy (MBE).

Figure 4 shows the refractive index at 630 nm as function of the thickness for films deposited at 500 and 650°C, from this figure, it is observed that the refractive index increases with thickness and with deposition temperature in the range of 1.55–1.75 in all cases. This behavior is most likely associated with the formation of an interfacial layer of silicate species and/or silicon oxide during the deposition process which has a low refractive index, thus the effective refractive index of the whole layer is lowered, especially for the thinner films. Figure 5 shows the refractive index for films with thicknesses in the range of 29–33 nm, as a function of deposition temperature. It is observed that the refractive indexes are in the range of 1.700–1.755 for these thicknesses, being consistently higher for the LA2 samples and for large deposition temperatures. These values are within the range of 1.66 and 1.836, which are the refraction indexes for aluminum oxide and lanthanum oxide respectively.[6,26] Also the behavior of the refrac-

Downloaded on 2016-09-12 to IP 130.203.136.75 address. Redistribution subject to ECS terms of use (see ecsdl.org/site/terms_use) unless CC License in place (see abstract).
IPR2025-00845
Apple-Sony EX1080 Page 3

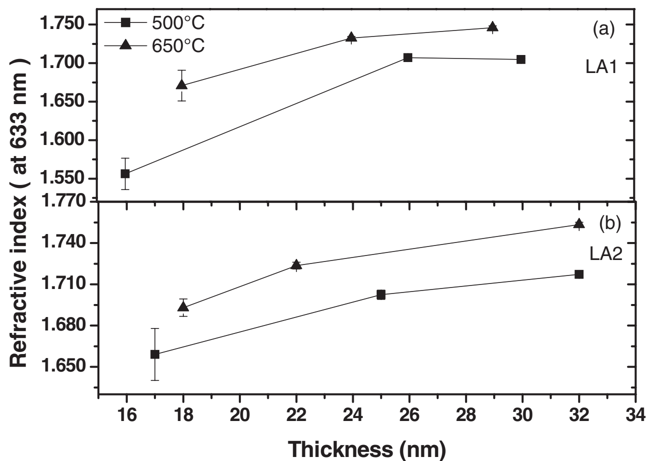

Figure 4. Refractive index as a function of the thickness for films deposited at 500 and 650°C.

tion index is consistent with the SIMS results (Fig. 3) which show that incorporation of lanthanum in the films is favored by larger deposition temperatures. More specifically, the refractive index values obtained are consistent with those reported for $La_{0.5}Al_{1.5}O_3$ and $La_{0.9}Al_{1.1}O_3$ films with a refractive index of 1.73 and 1.8, respectively.[2]

Figure 6 show cross section STEM micrographs in brightfield for LA1 and LA2 films deposited at 650°C. The films have a smooth surface in agreement with the AFM measurements. In both cases, the films remain amorphous at 650°C. The films present an interfacial layer (IL) with the silicon substrate of clear contrast, which suggests a silica rich composition. The thickness of the IL seems to be larger for LA2 (Fig. 6b) compared with LA1 (Fig. 6a). SIMS measurement suggests that the IL layer is composed by (Al, La)-Silicate species (see Fig. 3). The upper layer, with higher density, is composed by La and Al oxides according with the SIMS measurement. The presence of an IL in La related oxide thin films have been observed for $LaScO_3$, $La_xZr_{1-x}O_{2-\delta}$.[27,28]

Electrical characteristics such as capacitance vs. voltage and current density vs. applied electric field were carried out on MOS structures incorporating the LA films. Figure 7 shows typical 1 MHz and quasi-static capacitance vs. voltage characteristics for LA1 and LA2 films deposited at 500°C. The dielectric constant, obtained from the accumulation capacitance value, was in the range of 5.2 – 10 for films with a thickness in the 30 – 43 nm range. These values are

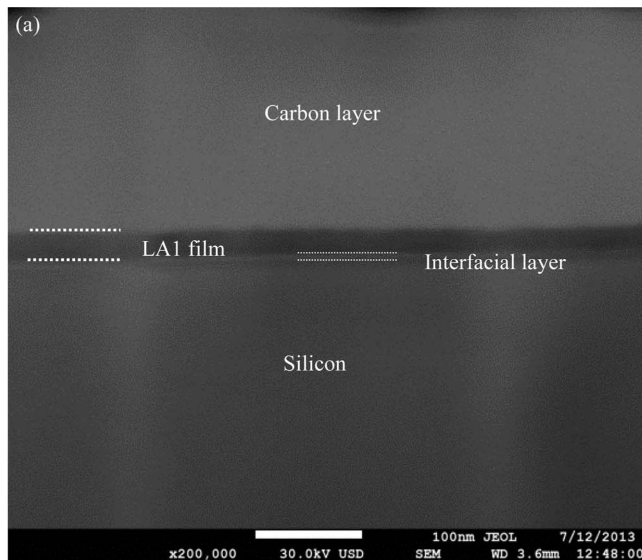

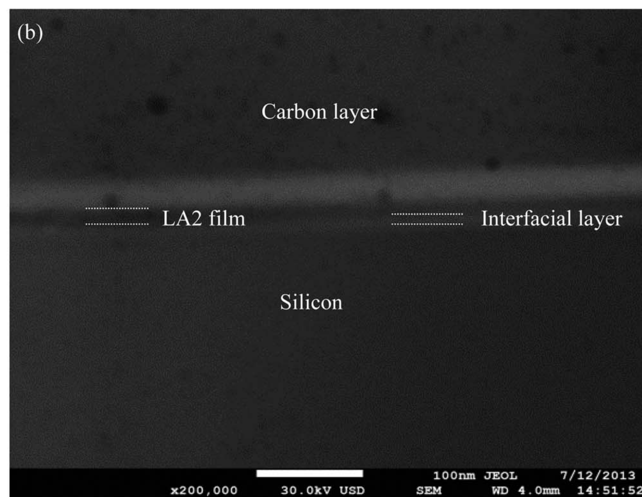

Figure 6. Cross section image for samples deposited at 650°C.

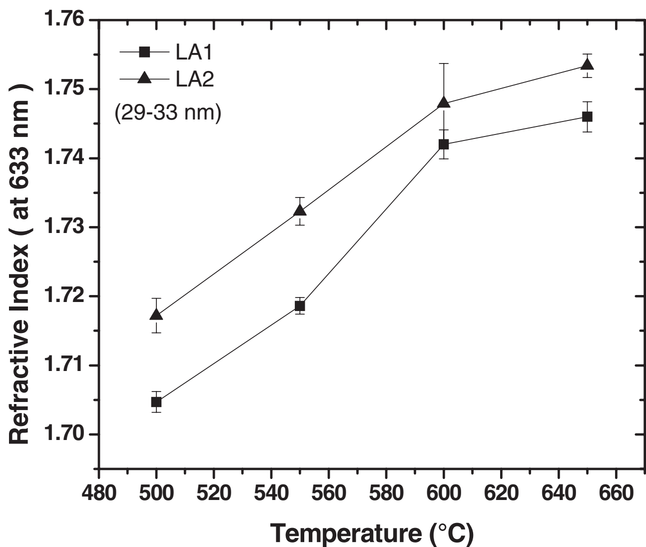

Figure 5. Refractive index as a function of the deposition temperature.

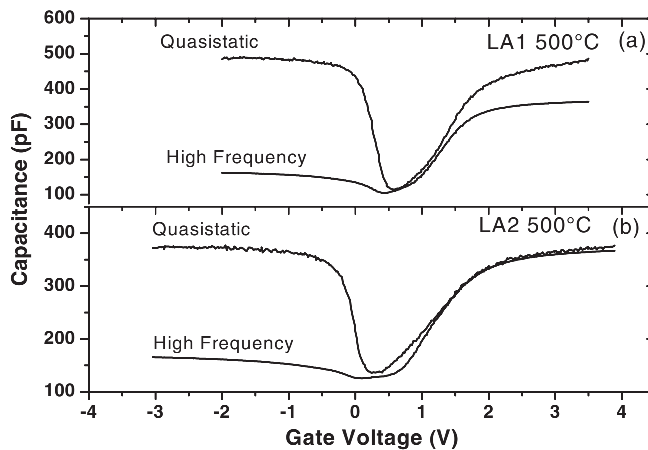

Figure 7. High frequency (1 MHz) and quasi-static capacitance vs. gate voltage for a MOS structure for films deposited at 500°C.

IPR2025-00845
Downloaded on 2016-09-12 to IP 130.203.136.75 address. Redistribution subject to ECS terms of use (see ecsdl.org/site/terms_use) unless CC License in place (see abstract).
Apple-Sony EX1080 Page 4

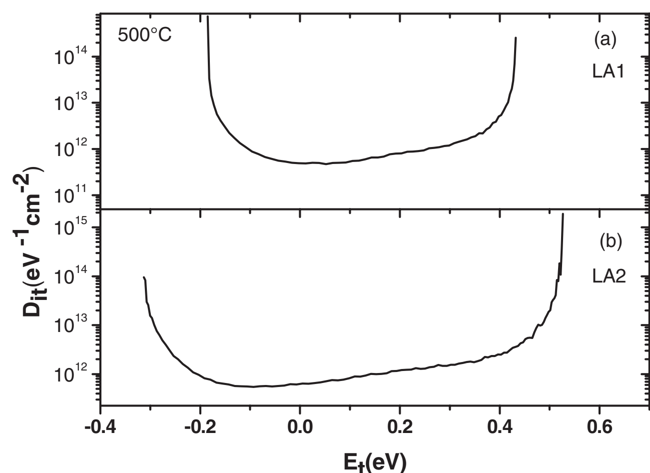

Figure 8. Typical curve of the interface trap density as a function energy measured from the silicon midgap for films deposited at 500°C.

low in comparison with those reported in Lanthanum aluminate and $La_xAl_yO_z$ films deposited by molecular-beam deposition and ALD, respectively,[7,29] and close with the reported in Lanthanum-aluminum oxide and La_xAl_yO films deposited by ALD and MOCVD[24,30] which showed the formation of an interfacial layer. The smallest dielectric constant value was obtained for LA2 at the highest deposition temperature (650°C). The low dielectric constant is correlated with the formation of an interface layer with a lower dielectric constant. In general, the LA films present negligible flatband voltage shift in comparison with those Al_2O_3 thin films deposited by ultrasonic spray pyrolysis,[6] this behavior could be attributed to the presence of La, which reduce the presence of positive charge inside the dielectric films. Figure 8 shows a typical curve of the interface trap density for LA films deposited at 500°C obtained from the 1 MHz and quasistatic capacitance curves (Fig. 7). The interface trap density at midgap was found to be of the order of 10^{11}-10^{12} ev^{-1} cm^{-2} for films deposited at 500°C. The interface trap density increases for larger deposition temperatures in both cases, this behavior could be related with the reactivity on the Si substrate since the formation of (Al, La)-silicates at the interface could be origin of these interface traps. This is confirmed by SIMS measurement of the interface thickness in which has been determined that higher temperature results in thicker interface layers. The typical ramp I-V curves for all deposition temperatures studied are shown in Figure 9. It is observed that for electric fields

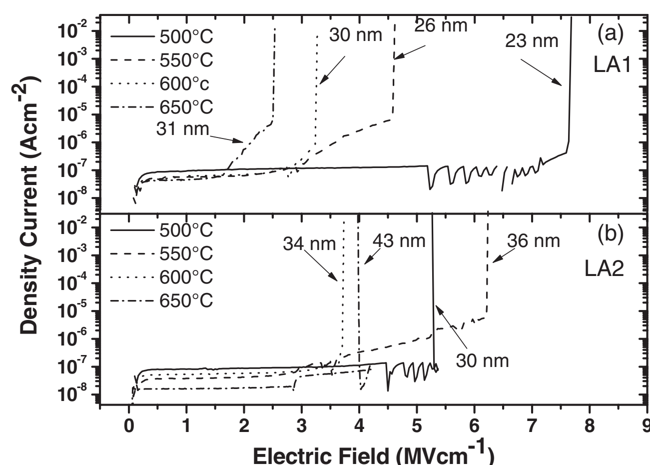

Figure 9. Current density vs electric field as function of the deposition temperature.

below of 2 $MVcm^{-1}$ the current density value is of the order of 10^{-8}-10^{-7} Acm^{-2} and it is due to a displacement current associated with the voltage ramp applied to the MOS structure in order to obtain the current versus voltage characteristics. At electric fields higher than 2 $MVcm^{-1}$ a real electron current (Fowler-Nordheim tunneling current) across of dielectric films of the order of 10^{-7}-10^{-6} Acm^{-2} is observed, and a destructive breakdown of the films is observed for electric fields higher than 2.4 $MVcm^{-1}$. In general, it is observed that films deposited at the lowest temperatures (500 and 550°C) show the best insulating characteristics with a breakdown field in the range of 4.5 – 7.6 $MVcm^{-1}$. The reduction of the breakdown field observed for films deposited at higher temperatures (600 and 650°C) is not clearly understood and further experimentation is required to be able to address this point properly. In general these films show better insulating characteristics than La_2O_3 and Al_2O_3, deposited by reactive radio-frequency sputtering and pulsed ultrasonic spray pyrolysis[15,31] and similar to those reported for lanthanum-aluminum oxide synthetized by atomic layer deposition.[2,29] It should be mention that the films in the current paper are much thicker than typical ALD films, since thicker films could be expected to show lower current leakage and direct comparison between the results for these two techniques should be taken with the caution.

Conclusions

The optical, structural and electrical characteristics of lanthanum-aluminum oxide thin films deposited by ultrasonic spray pyrolysis on silicon (100) substrates from lanthanum nitrate and aluminum acetylacetonate have been reported. It was observed that the incorporation of lanthanum in the films is favored by high deposition temperature as the refractive index behavior and the EDS studies indicate. The STEM studies on cross section structures showed the formation of a interfacial layer formed during the deposition process. SIMS measurements suggest that this layer is formed by (Al, La)-Silicate species. In general, high density films as reflected by the high refractive index values (in the 1.7 to 1.755 range, at the 633 nm wavelength), have been obtained with a low cost technique such as ultrasonic spray pyrolysis. The films were amorphous up to the highest deposition temperature studied 650°C, this characteristic together with the smooth (low roughness) surface led to films with high breakdown fields. The highest dielectric constant of the films, obtained from CV measurement was 10, the formation of an interface layer is responsible for the reduced value. The interface trap density was in the range of 10^{11}-10^{12} ev^{-1} cm^{-2}.

Acknowledgments

The authors would like to acknowledgement the technical assistance of M. Guerrero, R.J Fragoso-Soriano and A.B Soto. A. N. Meza-Rocha was supported by CONACyT-Mexico. The authors appreciate the cross section sample preparation and the STEM analysis to Dr. Hugo Martínez from Centro de Nanociencias y Micro-Nanotecnología del IPN.

References

1. G. D. Wilk, R. M. Wallace, and J. M. Anthony, *J. Appl. Phys.*, **89**, 5243 (2001).
2. Booyong S. Lim, Antti Rahtu, Philippe de Rouffignac, and Roy G. Gordon, *Appl. Phys. Lett.*, **84**, 3957 (2004).
3. Hei Wong, B. L. Yang, K. Kakushima, P. Ahmet, and H. Iwai, *Vacuum*, **86**(7), 929 (2012).
4. Yi Zhao, Masahiro Toyama, Koji Kita, Kentaro Kyuno, and Akira Toriumi, *Appl. Phys. Lett.*, **88**, 072904 (2006).
5. X. B. Lu, Z. G. Liu, X. Zhang, R. Huang, H. W. Zhou, X. P. Wang, and B.-Y. Nguyen, *J. Phys. D*, **36**, 3047 (2003).
6. M. Aguilar-Frutis, M. Garcia, and C. Falcony, *Appl. Phys. Lett.*, **72**, 1700 (1998).
7. L. F. Edge, D. G. Schlom, P. Sivasubramani, R. M. Wallace, B. Holländer, and J. Schubert, *Appl. Phys. Lett.*, **88**, 112907 (2006).
8. S. Carmona-Tellez, J. Guzman-Mendoza, M. Aguilar-Frutis, G. Alarcon-Flores, M. Garcia-Hipolito, M. A. Canseco, and C. Falcony, *J. Appl. Phys.*, **103**, 034105 (2008).

IPR2025-00845
Downloaded on 2016-09-12 to IP 130.203.136.75 address. Redistribution subject to ECS terms of use (see ecsdl.org/site/terms_use) unless CC License in place (see abstract).
Apple-Sony EX1080 Page 5

9. G. Alarcón-Flores, M. Aguilar-Frutis, C. Falcony, M. García-Hipolito, J. J. Araiza-Ibarra, and H. J. Herrera-Suárez, *J. Vac. Sci. Technol. B*, **24**, 1873 (2006).
10. Dainius Perednis and Ludwig J. Gauckler, *Journal of Electroceramics*, **14**, 103 (2005).
11. Pramod S. Patil, *Materials Chemistry and Physics*, **59**, 185 (1999).
12. A. N. Meza-Rocha, E. Zaleta-Alejandre, R. Balderas, Z. Rivera, M. L. Perez-Arrieta, and C. Falcony, *ECS Trans.*, **41**(9), 183 (2011).
13. *Handbook of Deposition Technologies for Films and Coatings, Science, Application and Technology*, Peter M. Martin (Elsevier, 2010 third edition), 339-344.
14. Sang-Woo Kang and Shi-Woo Rhee, *Journal of The Electrochemical Society*, **149**(6), C345 (2002).
15. S. Carmona-Tellez, C. Palacio, S. Gallardo, Z. Rivera, J. Guzman-Mendoza, M. Aguilar-Frutis, M. Garcia-Hipolito, G. Alarcon-Flores, and C. Falcony, *ECS Trans.*, **25**(6), 179 (2009).
16. S. Y. No, D. Eom, C. S. Hwang, and H. J. Kim, *J. Appl. Phys.*, **100**, 024111 (2006).
17. A.-E. Gobichon, J.- P. Auffrédic, and D. Louer, *Solid State Ionic*, **93**, 51 (1997).
18. M. Aguilar-Frutis, M. Garcia, C. Falconya, G. Pleschd, and S. Jimenez-Sandoval, *Thin Solid Films*, **389**, 200 (2001).
19. W. F. Xiang, Y. Z. Liu, H. B. Lu, L. Yan, M. He, and Z. H. Chen, *Thin Solid Films*, **515**, 2722 (2006).
20. D. Eom, C. S. Hwang, H. J. Kim, M.-H. Cho, and K. B. Chung, *Electrochemical and Solid-State Letters*, **11**(7), G33 (2008).
21. Q.-Y. Shao, A.-D. Li, J.-B. Cheng, H.-Q. Ling, D. Wu, Z.-G. Liu, N.-B. Ming, C. Wang, H.-W. Zhou, and B.-Y. Nguyen, *Appl. Phys. A*, **81**, 1181 (2005).
22. T. M. Klein, D. Niu, W. S. Epling, W. Li, D. M. Maher, C. C. Hobbs, R. I. Hegde, I. J. R. Baumvol, and G. N. Parsons, *Applied Physics Letters*, **75**, 4001 (1999).
23. Haruhiko Ono and Tooru Katsumata, *Applied Physics Letters*, **78**, 1832 (2001).
24. S.-Y. Cha, H.-J. Kim, and D.-J Choi, *Journal Ceramic Processing Research*, **12**, 57 (2011).
25. D. Y. Medina, S. Orozco, I. Hernandez, R. T. Hernandez, and C. Falcony, *Journal of Non-Crystalline solids*, **357**, 3740 (2011).
26. Weiming He, Steven Schuetz, Raj Solanki, John Belot, and James McAndrew, *Electrochemical and Solid-State Letters*, **7**(7), G131 (2004).
27. Hongtao Wang, Jun-Jieh Wang, Roy Gordon, Jean-Sébastien M. Lehn, Huazhi Li, Daewon Hong, and Deo V. Shenai, *Electrochemical and Solid-State Letters*, **12**(4), G13 (2009).
28. D. Tsoutsou, L. Lamagna, S. N. Volkos, A. Molle, S. Baldovino, S. Schamm, P. E. Coulon, and M. Fanciulli, *Appl. Phys. Lett.*, **94**, 053504 (2009).
29. Su Young Kim, Hyuk Kwon, Sang Jin Jo, Jeong Sook Ha, Won Tae Park, Dong Kyun Kang, and Byong-Ho Kimb, *Appl. Phys. Lett.*, **90**, 103104 (2007).
30. K. Kukli, M. Ritala, V. Pore, M. Leskelä, T. Sajavaara, R. I. Hedge, D. C. Gilmer, P. J. Tobin, A. C. Jones, and H. C. Aspinall, *Chem. Vap. Deposition*, **12**, 158 (2006).
31. T.-M. Pan, C.-L. Chen, W.-W. Yeh, and W.-J. Lai, *Electrochemical and Solid-State Letters*, **10**, H101 (2007).

IPR2025-00845
Downloaded on 2016-09-12 to IP 130.203.136.75 address. Redistribution subject to ECS terms of use (see ecsdl.org/site/terms_use) unless CC License in place (see abstract).
Apple-Sony EX1080 Page 6